Electrical conductivity of a tight-binding hard-sphere model for hot fluid metals

P. Tarazona,[1] E. Chacón,[2] J. A. Vergés,[2] M. Reinaldo-Falagán,[1] E. Velasco,[1] and J. P. Hernandez[3]
[1]*Física Teórica de la Materia Condensada (C-V) Universidad Autónoma de Madrid, E-28049 Madrid, Spain*
[2]*Instituto de Ciencia de Materiales de Madrid, CSIC, E-28049 Madrid, Spain*
[3]*Department of Physics and Astronomy, University of North Carolina, Chapel Hill, North Carolina 27599-3255, USA*
(Received 29 March 2004; revised manuscript received 3 September 2004; published 21 January 2005)

Hot fluid metals are represented using a tight-binding hard-sphere model. Various treatments of the electrical conductivity of those disordered systems are presented and results are compared for equilibrium ionic configurations near the liquid-vapor phase coexistence. The configurations are obtained from self-consistent Monte Carlo simulations, with the cohesive energy being due to exact calculations of the valence electron delocalization. The disorder in the electronic hopping elements arises from that of the ionic positions, since the hopping is assumed to decay exponentially with distance. Calculated values of the electrical conductivity are found to span several orders of magnitude along the liquid-vapor coexistence curve, from typical metallic values in the low-temperature dense liquid metal, to a percolation-limited transition, to an insulator on the vapor branch. We compare the results based on the Kubo-Greenwood treatment, formulated appropriately for the model, with those of a "mesoscopic" approach based on the Green's function method for the quantum-coherent transport between two voltages leads, and examine results from two versions of the randomized phase model, which assumes a rapid decay of the quantum coherence. The various conductivity results are also compared with the experimental data for cesium.

DOI: 10.1103/PhysRevB.71.024203 PACS number(s): 72.15.Cz, 71.30.+h, 72.60.+g

I. INTRODUCTION

Electrical conductivity in disordered systems is a subject of interest in many different fields of condensed matter physics, microelectronics, and nanotechnology. Theoretical techniques developed to study this problem range from the semiclassical formalism based on the Boltzmann equation to the nonequilibrium Green's function method in the Keldysh formalism; they have been applied to empirical models for the disorder, treated as a frozen framework on which the electronic properties are calculated. Fluid metals contrast with solid-state devices in many respects; for example, simple estimates of the mean free path in such fluids give a coherence length comparable to the nearest-neighbor distance,[1] so the effects of quantum interference should have much less relevance in such materials than in the case of low-temperature solid devices. Moreover, in fluids, the strong disorder produced by the ionic potentials acting on the electrons cannot be modeled as a frozen random distribution, since the valence electronic energy produces effective ion-ion interactions and leads to strongly correlated ionic positions, which have to be treated self-consistently with the electronic properties.

Simple lattice[2] and off-lattice models[3] were at first used to explore the properties of monovalent fluids in which the electronic delocalization produces a vapor-liquid phase transition similar to that observed in the alkali-atom fluids.[4] The tight-binding (TB) hard-sphere (HS) model is the simplest one which yields most of the qualitative aspects observed in the phase diagram of the alkalis. Solid, liquid, and vapor phases appear from the combined effects of the ionic-packing entropy, represented using a system of hard spheres of diameter d_{HS}, and the cohesive free energy of (noninteracting) electrons appropriately delocalized over the (half-filled) band obtained by using a tight-binding orbital on each ion. The hopping between orbitals associated with ions at positions $\mathbf{r}_i$ and $\mathbf{r}_j$ is taken, in this work, to decay exponentially with the distance $r_{ij}=|\mathbf{r}_i-\mathbf{r}_j|$, $t_{ij}=t_0\exp[-\alpha(r_{ij}-d_{\mathrm{HS}})]$. The parameters d_{HS} and t_0 give scaling units for distance (density) and energy (temperature) in the system, so they may be trivially varied to fit experimental data for the critical point of different alkali-atom fluids. The reduced exponential decay parameter of the hopping elements $\alpha^*=\alpha d_{\mathrm{HS}}$ is the only nontrivial one determining the phase diagram. The shape of the liquid-vapor coexistence curve, as a function of that parameter, was explored in other work, using either a combination of Monte Carlo (MC) simulations and effective glue-model interactions[3] or directly, with the MC simulations based on the exact evaluation of the electronic energies.[5] The choice $\alpha^*=2$, used in this paper, is the one for which the phase diagram of the TB-HS model resembles those obtained experimentally for cesium, rubidium, and potassium.[4]

In this paper, we center our attention on the calculation of the electrical conductivity (σ) near the liquid-vapor coexistence curve. Experimental results, cited in Refs. 6 and 7 and obtained by Ref. 8, show that the alkali fluids remain metallic on lowering the density until the upper part of the vapor branch is reached, with a monotonic decay of σ. For cesium, the conductivity is measured to have a value of $\sigma=3.3\times10^3$ S/cm (where S=Siemens=Ω^{-1}) in the dense liquid metal, at a density of $\rho=1.2$ g/cm^3. On reaching the critical density $\rho_c=0.379$ g/cm^3, the conductivity has decreased by more that a factor 10, and has again decreased by another order of magnitude to $\sigma=3.1\times10^1$ S/cm, at $\rho=0.16$ g/cm^3, well within the vapor branch but still at a fairly high temperature. The eventual transition to an insulating molecular gas, predicted in theoretical models of electrons in disordered media,[6,9] is hidden by the effects of other conduction mechanisms, for instance, those associated with the formation of charged clusters; also, accurate experimental mea-

surements of very low conductivities in a hot and reactive alkali vapor are unavailable due to the experimental difficulties. We shall present a quantitative comparison of conductivity results based on the TB-HS model with the above experimental data, beyond the qualitative one already contained in previous work. Further, in this paper, we consider a variety of theoretical treatments in order to improve the understanding of the metal-insulator transition in disordered model systems in which the characteristics of the disorder are self-consistently controlled by the electronic energies, rather than being determined by frozen empirical distributions.

In previous work,[3] we discussed effects on the electrical conductivity due to clustering and inhomogeneities in structure arising, within the TB-HS model, from the electronically induced positional correlations among ions. These effects already account for the metal-nonmetal transition, in the moderately low density vapor phase, without demanding a dominant role for electron-electron interactions; thus, such considerations qualitatively change early predictions. We showed that, even in the absence of any electron-electron interaction, correlations among the ionic positions cause the conductivity of the TB-HS model to decrease monotonically with decreasing density until the vapor is extremely dilute and the density is well below that at which data is available; it is only then that electron-electron interactions become a dominant effect. In contrast, early work ignored the correlations among ionic positions, induced by the electronic energy, consequently it was compelled to require a sufficiently strong effect of electron-electron interactions to avoid an increasing electrical conductivity as the density decreases, even in the moderately low density vapor. That unphysical increase arose from the fact that such an uncorrelated structural assumption caused isolated atoms to become more prevalent as density decreased and, even at moderate vapor densities, their increasing prevalence dominated the conductivity through their rapidly increasing electronic density of states at the Fermi energy.[6]

In the present study, we have found no qualitative differences in structural properties arising from basing the simulations on the exact,[5] rather than the glue-derived energies;[3] thus, the previous discussion remains valid in that respect. However, it seems useful to compare the results of various theoretical approximations for determining the electrical conductivity, in order to understand which features are the most important ones in these systems. Thus, we consider the Kubo-Greenwood description of conductivity,[10] in more generality than the previously used random phase approximation due to Hindley,[11] and also obtain results using a "mesoscopic" Kubo treatment. Section II presents the bases for these theoretical methods. Then, in Sec. III, we undertake the quantitative comparison among the results for $\sigma(\rho)$, along the vapor-liquid coexistence curve of the TB-HS model, using various theoretical approaches, and also include a comparison to experimental data for cesium (a typical and well studied alkali-atom fluid). A conclusions section closes the paper.

II. ELECTRICAL CONDUCTIVITY TECHNIQUES

The linear electronic transport properties of a disordered system should be described by the nonlocal conductivity tensor[12] $\sigma(\mathbf{r},\mathbf{r}')$, which relates the electric field $\mathbf{E}$ at any point to the induced current density at any other point

$$\mathbf{j}(\mathbf{r}) = \int d^3\mathbf{r}'\,\sigma(\mathbf{r},\mathbf{r}')\cdot\mathbf{E}(\mathbf{r}'). \tag{1}$$

The assumption of a uniform electric field over a macroscopic (or mesoscopic) sample leads to the definition of a local conductivity to be used in Ohm's law $\mathbf{j}(\mathbf{r})=\overline{\sigma}(\mathbf{r})\cdot\mathbf{E}$, with

$$\overline{\sigma}_{\mu\nu}(\mathbf{r}) = \int d^3\mathbf{r}'\,\sigma_{\mu\nu}(\mathbf{r},\mathbf{r}'), \tag{2}$$

and the indices (μ,ν) running over the three Cartesian components. The diagonal terms give the macroscopic conductance $G=\overline{\sigma}_{\mu\mu}A/L$ for homogeneous samples, of length L along the direction μ of the voltage difference and with a transverse area A.

The same assumption, a uniform electric field over the sample, leads to the Kubo-Greenwood formula for the mean tensor elements of the local conductivity, evaluated from the current-current correlations between the atom pairs (i,j) and (k,l), appropriate to a hopping model, in term of the eigenenergies E_n and the participation of each atom $\phi_n(i)$ to the eigenfunction[13]

$$\overline{\sigma}^{\mathrm{KG}}_{\mu\nu} = -\frac{2\pi e^2}{\Omega\hbar}\left\langle \sum_{m\neq n}\frac{\partial f}{\partial E_m}\left[\sum_{i,j}\phi^*_m(i)\phi_n(j)(\mathbf{r}_i-\mathbf{r}_j)\cdot\mathbf{u}_\mu t_{ij} \times \sum_{k,l}\phi_m(k)\phi^*_n(l)(\mathbf{r}_k-\mathbf{r}_l)\cdot\mathbf{u}_\nu t_{kl}\right]\delta(E_m-E_n)\right\rangle; \tag{3}$$

the average over configurations is denoted by $\langle\cdots\rangle$, $\mathbf{u}_\mu$ is the unit vector in the μ direction, f is the Fermi-Dirac distribution function, and $\Omega=\langle N\rangle/\rho$ is the volume of the system.

However, nonlocal quantum effects and the requirement of charge conservation [$\nabla\cdot\mathbf{j}(\mathbf{r})=0$, for stationary states] may lead to long-ranged nonlocal dependences of $\sigma(\mathbf{r},\mathbf{r}')$, frustrating the definition of the local conductivity tensor in Eq. (2) and the Ohmic dependence of the conductance with the sample size.[12] Such an effect is already clear in Eq. (3), where the electronic (hopping) currents at distant bonds (i,j) and (k,l) can contribute to $\overline{\sigma}^{\mathrm{KG}}$ and spoil the intrinsic (size independent) character of the conductivity. It is well known that such effects cause the conductance of ordered mesoscopic systems at very low temperatures to be nonohmic, since all the resistance appears at the contacts between the sample and the voltage leads to macroscopic reservoirs. In the "mesoscopic" version of the Kubo formula, the nonlocal character of $\sigma(\mathbf{r},\mathbf{r}')$ is taken into account through a direct evaluation of the total conductance of the system, comprising the sample and the external contacts to macroscopic leads. That total conductance is expressed in terms of the components of the velocity operator and the Green's function as[12]

$$G = 2\frac{e^2}{h}\mathrm{Tr}[(i\hbar\hat{v}_\mu)\mathrm{Im}\,\hat{\mathcal{G}}(E_F)(i\hbar\hat{v}_\mu)\mathrm{Im}\,\hat{\mathcal{G}}(E_F)], \quad (4)$$

where $\hat{v}_\mu$ is the velocity operator and $\mathrm{Im}\,\hat{\mathcal{G}}(E)$ is obtained from the advanced (a) and retarded (r) Green's functions using

$$\mathrm{Im}\,\hat{\mathcal{G}}(E_F) = \frac{1}{2i}[\hat{\mathcal{G}}^r(E_F) - \hat{\mathcal{G}}^a(E_F)] = -\pi\delta(E-\hat{\mathcal{H}}). \quad (5)$$

Finite temperature effects may be explicitly included using an integral over the conductance contribution from states with specified energy

$$G = -\int dE \frac{df(E)}{dE} G(E). \quad (6)$$

The results of this approach, within our TB description of the electrons, are described below.

There are two different effects which may cancel quantum nonlocal characteristics of $\sigma(\mathbf{r},\mathbf{r}')$ and recover the Ohmic behavior $G=\sigma A/L$, with a well-defined intrinsic conductivity. First, the quantum decoherence of the electronic wave functions, produced by the atomic movements, will introduce random phases between the wave-function products $\phi^*(i)\phi(j)$ and $\phi^*(k)\phi(l)$ and cancel, in Eq. (3), contributions from hopping between distant pairs (k,l) and (i,j). This effect may be represented by a decoherence length, λ_D in Chambers formula[14]

$$\langle\sigma^{\mathrm{Ch}}_{\mu\nu}(\mathbf{r},\mathbf{r}')\rangle = \frac{3}{4\pi}\frac{\sigma_D(\mathbf{r}-\mathbf{r}')_\mu(\mathbf{r}-\mathbf{r}')_\nu}{|\mathbf{r}-\mathbf{r}'|^4\lambda_D}\exp\left(-\frac{|\mathbf{r}-\mathbf{r}'|}{\lambda_D}\right), \quad (7)$$

where $\sigma_D(\mathbf{r},\mathbf{r}')$ should be a smooth function of $|\mathbf{r}-\mathbf{r}'|$. In our model for hot fluid metals, we might assume that λ_D is small compared with the HS diameter d_{HS}, which leads directly to the randomized phase model (RPM) of Hindley:[11]

$$\overline{\sigma}^{\mathrm{RPM}}_{\mu\mu} = -\frac{2\pi e^2}{\Omega\hbar}\left\langle \sum_{m\neq n}\frac{\partial f}{\partial E_m}\sum_{i,j}|\phi_m(i)|^2|\phi_n(j)|^2 \times[(\mathbf{r}_i-\mathbf{r}_j)\cdot\mathbf{u}_\mu t_{ij}]^2\delta(E_m-E_n)\right\rangle, \quad (8)$$

so that only the contributions with $(i,j)=(k,l)$ in Eq. (3) survive. Then the remaining contribution from the sum over pairs, where the pair distance is limited by the decaying hopping element, gives a term proportional to N and to the system volume Ω in the denominator.

Even in absence of the above decoherence effect, there is an alternative way to recover the Ohmic behavior based on the strong disorder of the fluid configurations. The variety of disordered equilibrium configurations in the fluid leads to strong fluctuations of the wave-function amplitudes and cancels the averaged cross contributions from distant pairs $|\mathbf{r}_i-\mathbf{r}_k|, |\mathbf{r}_j-\mathbf{r}_l| \gg d_{\mathrm{HS}}$ in Eq. (3). This is the way, as discussed in the next section, in which the Kubo-Greenwood formulation $\overline{\sigma}^{\mathrm{KG}}_{\mu\mu}$, when averaged over equilibrium fluid configurations, recovers the intrinsic character of a macroscopic conductivity, one which would be lost in a perfectly ordered crystal at $T=0$. The same effect results in the "mesoscopic" application of the Kubo formalism, with Green's functions linking the sample to the macroscopic reservoirs. When Eq. (4) is applied to a single fixed ionic configuration, the conductance G is determined by the area of the contacts to the metallic leads, rather than by the sample geometry. But, on averaging over typical fluid configurations, obtained in our MC simulations, such a formulation also recovers the ohmic dependence with sample size and produces a well defined mean conductivity $\langle\sigma\rangle^{\mathrm{KG}} \equiv LG/A$, almost independent of the sample geometry.[15] We shall maintain the notation of $\overline{\sigma}$ for results based on the assumption of a local conductivity (2) and use $\langle\sigma\rangle$ for those obtained from the conductance of the full sample, the subindices $\mu\mu$ for the diagonal components of the tensor are eliminated in our application to statistically isotropic samples.

We expect that both disorder and decoherence are important in determining the conductivity of hot fluid metals. Our MC simulations for the TB-HS model provide a self-consistent description of the disorder at any point of the liquid-vapor phase diagram, and a comparison of results from the full Kubo-Greenwood result and the RPM version of Hindley gives a measure of the effects of quantum decoherence, fully neglected in Eq. (3) and assumed complete in Eq. (8). For dense fluids, the assumption of a uniform electric field over the sample should be appropriate. Hence, differences between the "macroscopic" Kubo-Greenwood formulation and its "mesoscopic" Green's function version will be small and are expected to be due to unrelated, more technical, causes as follows. Finite size effects in our MC samples require a finite width to be applied the delta function $\delta(E_m-E_n)$ in Eq. (3), to compensate for the discreteness of the energy spectrum; such a procedure is equivalent to defining the dc conductivity as the average of ac conductivities over a narrow range of small frequencies $\omega \sim t_0/(N\hbar)$. Similarly, the evaluation of sample conductances through Eq. (4) requires an explicit construction that attaches the simulated sample to metallic leads.[16] This requirement is implemented through small imaginary parts, in the Green's functions, that allow the evaluation of the sample conductance. The dependence of $\overline{\sigma}^{\mathrm{KG}}$ on the specific coarsening of frequencies in Eq. (3), and that of $\langle\sigma\rangle^{\mathrm{KG}}$ on the modeled contacts, are treated on an empirical basis which searches for the range of these parameters giving results which are fairly independent of the particular parameter choices.

In contrast, at the much lower densities corresponding to the vapor branch, results for $\overline{\sigma}^{\mathrm{KG}}$ may become very different from those extracted from the total conductance of the samples, using the "mesoscopic" Green's function treatment. When the sample has the strong inhomogeneity typical of fluids near the critical point, the electronic conduction is determined by the "easy paths" formed along the hopping bonds of clusters which percolate across the sample. Such a percolative character is preserved in the "mesoscopic" version of the Kubo formula, since the total conductance comes from the Green's functions linking the two leads through the electronic hopping in the sample. However, the macroscopic Kubo-Greenwood approach (3) neglects such percolative aspects of the conduction, given the assumption of uniform

electric field. This neglect corresponds to treating a network of classical resistors, with different resistors R_{ij}, as equivalent to a network in which all resistors are equal to $\overline{R}$, such that $1/\overline{R}$ is obtained from the mean value of the bond conductances G_{ij}. In contrast to such an approach, the consistent solution of Kirchhoff's equations, taking into account the different voltage drops at different networks links (i.e., the nonuniform electric field), leads to an effective averaging of G_{ij} for those links connected in parallel, while the relevant average is done directly over R_{ij} for those connected in series.

Obviously, the above problem again appears in $\overline{\sigma}^{\mathrm{RPM}}$. The approach used in our previous work, representing the conductance of a sample (using configurations obtained in our MC simulations) by that of a network of classical resistors R_{ij} between each atom pair, corresponds to an attempt to recover the percolative character of the conduction within the RPM scheme. Such an approach leads to results apparently more appropriate to fluid metals than those of averaging the perfect quantum coherence assumed in Eq. (4). To implement such a recovery, maintaining a quantitative description, we apply the Kubo-Greenwood generic argument to the microscopic conductance along the (i,j) bond between two nearby atoms. Thus associating $\sigma(\mathbf{r}_i,\mathbf{r}_j)$ with the direct local diffusion rate $D_{ij}\sim\langle \mathbf{v}_{ij}^2\rangle$, using a representation of the velocity operator in terms of the hopping elements as in (8), to obtain

$$\sigma_{\mu\mu}(\mathbf{r}_i,\mathbf{r}_j)\approx -\frac{2\pi e^2}{\Omega\hbar}\left\langle \sum_{m\neq n}\frac{\partial f}{\partial E_m}|\phi_m(i)|^2|\phi_n(j)|^2 \times[(\mathbf{r}_i-\mathbf{r}_j)\cdot\mathbf{u}_\mu t_{ij}]^2\delta(E_m-E_n)\right\rangle. \quad (9)$$

The assumption of strong decoherence, which cancels current-current correlations between separated bonds and hence allows Eq. (3) to be written as Eq. (8), implies that successive jumps along the hopping elements are incoherent, so that the transport properties of a configuration corresponds to that of a classical network of resistors, with values $1/R_{ij}\sim\sigma(\mathbf{r}_i,\mathbf{r}_j)$ between any pair of atoms with nonvanishing hopping elements. The proportionality factors, which in our previous work were hidden within a rescaling factor (the conductivity of the dense liquid), may be found quantitatively in order to precisely recover the expression (8) for $\overline{\sigma}^{\mathrm{RPM}}$, whenever the electric field is assumed to be homogeneous. That procedure yields

$$\frac{1}{R(r_{ij})}=\frac{1}{2}\xi_{ij}[t(r_{ij})]^2, \quad (10)$$

with ξ_{ij} given by

$$\xi_{ij}=\frac{2\pi e^2}{\hbar}\left[\sum_{m\neq n}\left(-\frac{\partial f}{\partial E_m}\right)|\phi_m(i)|^2|\phi_n(j)|^2\delta(E_m-E_n)\right]. \quad (11)$$

For each ionic configuration, Kirchhoff's laws are to be applied to the resistor network, with a potential difference between two opposing sides of a sample. The total conductance $G=I/\Delta V$ is averaged over ionic configurations along our MC simulations. Just as in the "mesoscopic" KG treatment, Ohm's law is then applied using $\langle\sigma\rangle\equiv(L_z-2l_c)G/A$, in terms of the transverse area A and the effective length of the system, excluding the voltage leads. We label the intrinsic conductivity given by this method as $\langle\sigma\rangle^{\mathrm{RPM}}$, since it corresponds to the macroscopic results of applying the RPM to the microscopic nonlocal conductance, but keeping the percolative character of the conduction over the full sample.

Both $\langle\sigma\rangle^{\mathrm{KG}}$ and $\langle\sigma\rangle^{\mathrm{RPM}}$ lack a contribution from isolated clusters, so samples without ionic structures which percolate between the two leads will have zero conductivity. Thus, there is a formal qualitative difference between conductivity results which use the full exponential decay $t_{ij}=t_0\times\exp[-\alpha(r_{ij}-d_{\mathrm{HS}})]$ of the hopping elements and those where (for simplicity) t_{ij} is truncated to zero beyond a cutoff r_{cut}. In the second case there is a true percolative transition at which $\langle\sigma\rangle$ becomes strictly zero, while for infinite-ranged hopping there can be no true percolative transition, so $\langle\sigma\rangle$ will never be strictly null. However, the previous studies, with $r_{\mathrm{cut}}=3.1d_{\mathrm{HS}}$, show that such differences only appear when $\langle\sigma\rangle$ is many orders of magnitude smaller than the experimentally accessible range. Thus, the difficulty of analyzing percolative transitions, with the small samples we used to obtain the electronic properties of our TB-HS model, prevents us from discussing that region. For all practical purposes, the drop of σ by more than six orders of magnitude with respect to its value in the dense liquid metal should be interpreted as the transition to a non-metallic vapor in the TB-HS model, the density at which this decrease has taken place is roughly independent of the value of the cutoff, for $r_{\mathrm{cut}}\geqslant 3.1d_{\mathrm{HS}}$.

Thus we have four different approaches to the electrical conductivity of our model system. All them estimate σ starting from the current-current correlations in the Kubo formula, with the exact wave functions of the TB Hamiltonian for each ionic configuration and a variety of ionic configurations representing statistical equilibrium. Two of the approaches, $\langle\sigma\rangle^{\mathrm{KG}}$ and $\overline{\sigma}^{\mathrm{KG}}$, assume perfect quantum coherence over a configuration, although the strong disorder of the fluid cancels the effects of such coherence (on averaging over equilibrium configurations) beyond microscopic distances and recovers Ohmic behavior for our sample sizes of a few hundred atoms.[15] The other two, $\langle\sigma\rangle^{\mathrm{RPM}}$ and $\overline{\sigma}^{\mathrm{RPM}}$, assume complete decoherence beyond a first-neighbor distance, so that the Ohmic character of the conduction will result even in perfectly ordered samples. On the other hand, $\overline{\sigma}^{\mathrm{KG}}$ and $\overline{\sigma}^{\mathrm{RPM}}$ assume the existence of a local conductivity, associated with the hypothesis of a uniform electric field, and calculate its average over the samples. The other two, $\langle\sigma\rangle^{\mathrm{KG}}$ and $\langle\sigma\rangle^{\mathrm{RPM}}$, are obtained from averaging the full sample conductance, which takes into account the percolative nature of the conduction process. For high system density we expect $\overline{\sigma}^{\mathrm{KG}}\approx\langle\sigma\rangle^{\mathrm{KG}}$ and $\overline{\sigma}^{\mathrm{RPM}}\approx\langle\sigma\rangle^{\mathrm{RPM}}$, while for low density $\langle\sigma\rangle^{\mathrm{KG}}$ and $\langle\sigma\rangle^{\mathrm{RPM}}$ will reflect the existence of a percolation transition, of quantum character in the former case and in terms of classical resistors in the latter one.

III. RESULTS FOR THE TB-HS MODEL

Conductivity calculations, using the four approaches, have been carried out for thermal equilibrium configurations of the TB-HS model with $\alpha^*=2$, in order to compare the various theoretical approaches among themselves and with experimental data for fluid cesium. To compare with experimental conductivity data as a function of density, a choice of our length unit is required: we use $d_{\mathrm{HS}}=4.7$ Å, a value which gave a good description of the structural properties of the experimental fluid near the normal melting point; the value of t_0 does not affect to the conductivity, as the choice of the energy unit is irrelevant to this magnitude.

Experimental conductivity data for cesium is available for "near-coexistence conditions"[6–8] and the model phase diagrams we have obtained, based on the exact[5] or glue-derived[3] energies, are quite similar, therefore conductivities were calculated for temperatures and densities "near" the model's phase coexistence, as described in what follows. For the conductivity calculations we choose equilibrium configurations obtained from NVT simulations using $N=256$ and exact electronic energies for the TB-HS model, with $\alpha^*=2$ and $r_{\mathrm{cut}}=3.1\ d_{\mathrm{HS}}$; however, temperatures and densities were chosen to correspond to the coexistence conditions obtained in our previous work (using glue-model derived energies, $N=1500$, and NVT-slab simulations). The conductivities from the various theoretical approaches were obtained, along the z direction, in a system with the geometry of a parallelepiped: $L_x=L_y=L$ and $L_z=2L$, with the dimensions chosen to correspond to N and the density. Further, as the sample sizes are small, the calculations were repeated for the alternative geometry of a cubic sample, to check whether the conductivity is Ohmic (independent of geometry); it was found that the ohmic limit had indeed been achieved for these system sizes, due to the strong disorder in the systems as analyzed below. Although the results were obtained using a cutoff in the hopping range at $r_{\mathrm{cut}}=3.1d_{\mathrm{HS}}$, it was determined that dispensing with the cutoff had little effect on the results (except extremely close to the percolation limit, a situation already discussed in previous work[3]). For each temperature and density, once the system was stabilized, MC simulations were carried out with 2×10^5 (or 4×10^5) MC steps. The conductivities were calculated for configurations obtained each 100 (or 200) steps, and each set of results averaged over the 2000 configurations. To obtain $\overline{\sigma}^{\mathrm{KG}}$ and $\overline{\sigma}^{\mathrm{RPM}}$ we used periodic boundary conditions in the three directions, the same procedure followed in evaluating the electronic energies for the MC simulations. However, for the other two approaches, based on the total conductance G of the sample, periodic boundary conditions were applied only for the transverse directions XY; in the Z direction, the voltage contacts at the two ends of the sample were chosen as any atom within slabs of width $l_c\approx d_{\mathrm{HS}}$, a size much smaller than the total sample length L_z but large enough to contain 8–10 ions. More precisely, we attached independent single-channel metallic wires to any of the atoms belonging to the contacts. The density of states of the leads roughly coincides with the Fermi-level density of states of the isolated sample.

Figure 1 exhibits the electrical conductivity results, as functions of density, in the units (S/cm) of the experimental

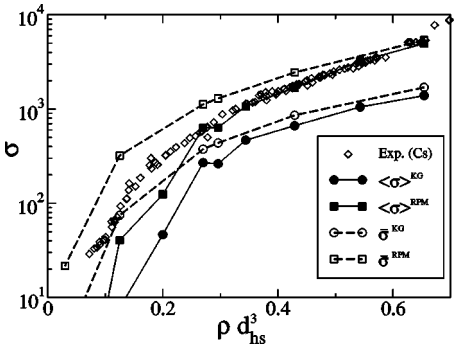

FIG. 1. Electrical conductivities (S/cm) along the coexistence curve of our model, obtained by averaging over configurations as described in the text. The diamonds represent experimental data for fluid cesium, close to coexistence. Circles show our quantum coherent results and squares our noncoherent ones. "Mesoscopic" results ($\langle\sigma\rangle$) are shown as filled symbols joined by solid lines, and macroscopic ones ($\overline{\sigma}$) as empty symbols joined by dashed lines. Lines are guides to the eye.

data. Notice that, in following the coexistence curve, the temperature changes nonmonotonically with density,[3,5] from $kT/t_0=0.10$, at the dense liquid metal ($\rho d_{\mathrm{HS}}^3\approx0.64$), to $kT/t_0=0.15$, at the critical point ($\rho d_{\mathrm{HS}}^3\approx0.15$), but then decreasing in the vapor branch as the density decreases. The figure also contains experimental data for expanded fluid cesium, cited elsewhere[6,7] and obtained by Franz,[8] ranging over the full liquid branch and the high density part of the vapor branch. Comparing the theoretical results among themselves shows that in the dense liquid there is a fair agreement between $\overline{\sigma}^{\mathrm{KG}}$ and $\langle\sigma\rangle^{\mathrm{KG}}$, and also between $\overline{\sigma}^{\mathrm{RPM}}$ and $\langle\sigma\rangle^{\mathrm{RPM}}$, as expected when the high connectivity of the hopping matrix makes essentially all paths percolative. Moreover, the agreement between $\overline{\sigma}^{\mathrm{KG}}$ and $\langle\sigma\rangle^{\mathrm{KG}}$ supports the technical details employed in our treatment of finite-size effects [i.e., the coarsening of the delta function in Eq. (3) and the inclusion of the imaginary self-energy in Eq. (4)], and gives witness to the fact that the disorder is strong enough to achieve Ohmic behavior within our system sizes. The use of the RPM assumption (both in $\overline{\sigma}^{\mathrm{RPM}}$ and in $\langle\sigma\rangle^{\mathrm{RPM}}$) causes in a systematic increase in the electrical conductivity, a multiplicative factor of approximately three over the Kubo-Greenwood or the "mesoscopic" Green's function approach with full quantum coherence. Thus, the off-site current-current correlations, neglected in the RPM, yield a substantial partial cancellation of the diagonal contribution ($i=k$ and $j=l$) in Eq. (3). However, the disagreement, reflected in the approximately constant multiplicative factor, between $\overline{\sigma}^{\mathrm{RPM}}$ and $\overline{\sigma}^{\mathrm{KG}}$ is a minor effect, compared to the strong variation of two orders of magnitude in $\overline{\sigma}$ along the liquid branch of the coexistence curve. Note that the simplicity of the TB-HS model could hardly be expected to give conductivities in more than semiquantitative agreement with experimental data. In this sense, we consider that the excellent agreement between the global-RPM conductivity $\langle\sigma\rangle^{\mathrm{RPM}}$ and the experimental data, over the full density range of liquid cesium, is probably accidental. Any improvement of the model, such as including a more realistic density of

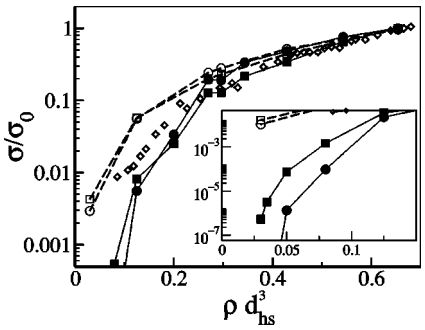

FIG. 2. As in Fig. 1, but now all conductivities are normalized to those obtained (in each calculation) at $\rho d_{\mathrm{HS}}^3 = 0.654$. Inset shows an enlarged view of the low density region.

states, might easily change all the theoretical predictions by a factor similar to the ratio between $\langle\sigma\rangle^{\mathrm{RPM}}$ and $\langle\sigma\rangle^{\mathrm{KG}}$.

In Fig. 2 we again present the electrical conductivity, but now the results of each method are normalized to its result (σ_0) at a common density in the dense liquid. This presentation allows a more robust comparison among the density dependences obtained from the different theoretical approaches and with that of the experimental results. The predictions of the two local versions ($\overline{\sigma}^{\mathrm{RPM}}$ and $\overline{\sigma}^{\mathrm{KG}}$) are very similar over the full density range, while those from the global versions ($\langle\sigma\rangle^{\mathrm{RPM}}$ and $\langle\sigma\rangle^{\mathrm{KG}}$) only differ appreciably very near to the percolation transition (see the inset). The experimental data in the near-critical density region seem to "split the difference," smoothing the rapid decay of $\langle\sigma\rangle^{\mathrm{RPM}}$ and $\langle\sigma\rangle^{\mathrm{KG}}$ in the vapor phase. An enhanced experimental conductivity in this density range may be expected from effects of charge transfer between clusters,[7,17] which are not taken into account in the HS-TB model. The percolation regime ($\rho d_{\mathrm{HS}}^3 \leqslant 0.1$, shown in the inset) is not really relevant for comparison with experiments, but it is of theoretical interest since it allows a comparison between quantum versus classical percolation. As expected, quantum percolation yields a lower conductivity that its classical counterpart, since it fully accounts for wave function localization which is only partially included in the RPM version. However, results for $\rho d_{\mathrm{HS}}^3 \leqslant 0.05$ are influenced by our use of the hopping cutoff, at $r_{\mathrm{cut}} = 3.1 d_{\mathrm{HS}}$, and have an uncontrolled bias due to finite-size effects in our samples.

We now shift the focus of the discussion to the intrinsically interesting theoretical problem of understanding the origin of the approximately constant discrepancy between $\overline{\sigma}^{\mathrm{RPM}}$ and $\overline{\sigma}^{\mathrm{KG}}$. This discrepancy is also related to the way in which disorder in the ionic positions produces intrinsic conductivities from theoretical formulations (3) and (4) which do not have an explicitly Ohmic behavior. To that end we present, in Table I, details of different contributions to the double sum (i,j) and (k,l) in Eq. (3), leading to $\overline{\sigma}^{\mathrm{KG}}$. The tabular results correspond to four different densities, from the dense liquid to the percolation threshold. At each density, we separate the contributions to Eq. (3) into five terms in which the "bond currents" are correlated differently. Notice that the contributions have the character of "directed bonds" due to the dot products in Eq. (3). A first term consists of pairs with $i=k$ and $j=l$; they give precisely the RPM result

TABLE I. Contributions to the double sums in Eq. (3) leading to $\overline{\sigma}^{\mathrm{KG}} = \overline{\sigma}^{\mathrm{RPM}} + \overline{\sigma}_X^{\mathrm{RPM}} + \overline{\sigma}^{\mathrm{AD}} + \overline{\sigma}_X^{\mathrm{AD}} + \overline{\sigma}^{N\text{-AD}}$ at four different coexistence densities. $\overline{\sigma}^{\mathrm{RPM}}$ is the summation of terms with $i=k$ and $j=l$ (RPM contribution), the electric current due to self correlation at each bond. $\overline{\sigma}_X^{\mathrm{RPM}}$ contains the terms with $i=l$ and $j=k$, as in $\overline{\sigma}^{\mathrm{RPM}}$ but exchanging the combination of wave functions. $\overline{\sigma}^{\mathrm{AD}}$ has terms with $i=k$ but $j\neq l$ (or equivalently $j=l$ but $i\neq k$), which correspond to the correlation between currents in adjacent bonds sharing a common site. $\overline{\sigma}_X^{\mathrm{AD}}$ has the terms with $i=l$ but $j\neq k$ (or equivalently $j=k$ but $i\neq l$), as in $\overline{\sigma}^{\mathrm{AD}}$ but exchanging the combination of wave functions. $\overline{\sigma}^{N\text{-AD}}$ consists of terms with $i\neq k$ but $j\neq l$, the contribution from the current correlations between nonadjacent bonds.

	$\rho d_{\mathrm{HS}}^3 = 0.654$	$\rho d_{\mathrm{HS}}^3 = 0.429$	$\rho d_{\mathrm{HS}}^3 = 0.2$	$\rho d_{\mathrm{HS}}^3 = 0.05$
$\overline{\sigma}^{\mathrm{KG}}$	1660	788	200	9.7
$\overline{\sigma}^{\mathrm{RPM}}$	4964	2259	652	60.3
$\overline{\sigma}_X^{\mathrm{RPM}}$	−98	−134	−108	−15.8
$\overline{\sigma}^{\mathrm{AD}}$	−7444	−2997	−667	−42.5
$\overline{\sigma}_X^{\mathrm{AD}}$	105	127	59	1.2
$\overline{\sigma}^{N\text{-AD}}$	4133	1533	264	6.5

(8) and correspond to the electric current self-correlation at each bond, their contribution to $\overline{\sigma}^{\mathrm{KG}}$ is, of course, always positive. A second term contains antiparallel pairs, terms with $i=l$ and $j=k$ in Eq. (3), which contribute with a negative sign, dominantly from the factor $(\mathbf{r}_i-\mathbf{r}_j)_\mu(\mathbf{r}_k-\mathbf{r}_l)_\mu$ (as the wave function contribution is not positive definite). This second contribution contains the "exchanged" combination of wave functions $\phi_m^*(i)\phi_n(j)\phi_m(j)\phi_n^*(i)$ instead of the "direct" one $\phi_m^*(i)\phi_n(j)\phi_m(i)\phi_n^*(j) = |\phi_m(i)|^2|\phi_n(j)|^2$; thus, they are excluded from the RPM approach. We find that this second contribution is approximately 20% of the RPM result for the rarefied vapor, but its relative weight is only about 2% for the dense liquid. A third set of terms consists in contributions from the terms with $i=k$ but $j\neq l$ (or equivalently $j=l$ but $i\neq k$), corresponding to the correlation between currents in adjacent bonds, sharing a common site, and having "head-to tail" orientation; the common site contributes with the "direct" (but not the "exchanged") combination of the wave functions. As seen in Table I, the averaged contribution, from these third set of terms, seems to be always negative and can be quite large, overwhelming the direct RPM contribution. In contrast, the fourth set of terms has the exchanged wavefunction combination for adjacent bonds; it appears to be always positive, but is too small to be of much importance. Finally, a fifth set of terms is the averaged contributions to $\overline{\sigma}^{\mathrm{KG}}$ from those bond pairs with $i\neq k$ and $j\neq l$, i.e., the contribution from the current correlations between distinct, nonadjacent, bonds; their contribution to the global sum is positive. The entire collection of terms conspires to a global result of an approximate ratio of $1/3$ between $\overline{\sigma}^{\mathrm{RPM}}$ and $\overline{\sigma}^{\mathrm{KG}}$, throughout the liquid range.

To seek a clearer explanation of the magnitudes and signs of the various contributions discussed in Table I, which are averaged over the disordered ionic positions, we explore the dependence of the above correlations with distance between the bonds. Also, such information is necessary to try to understand, in some detail, the source of the ohmic character of

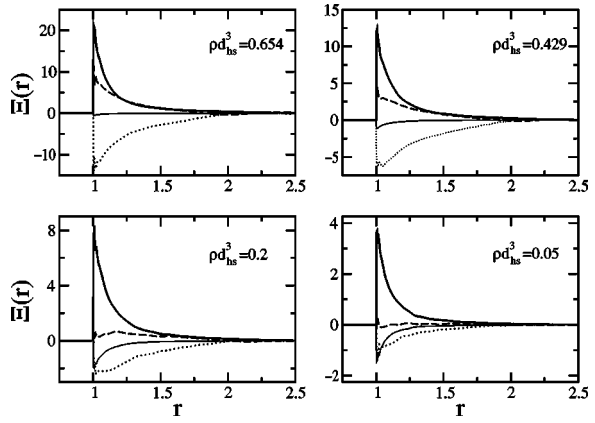

FIG. 3. Averaged radial distribution $\Xi(r)$ of various contributions to the double sums leading to $(\overline{\sigma}^{\mathrm{KG}})$, in terms of the distances. Broad solid line: $(\overline{\sigma}^{\mathrm{RPM}})$ RPM contribution, pairs with $i=k$ and $j=l$ in terms of r_{ij}. Thin solid line: $(\overline{\sigma}_X^{\mathrm{RPM}})$ exchanged bonds RPM contribution, pairs with $i=l$ and $j=k$ in terms of r_{ij}. Dotted line: $(\overline{\sigma}^{\mathrm{AD}}+\overline{\sigma}_X^{\mathrm{AD}})$ both adjacent-bond terms, pairs with $i=k$ but $j\neq l$ (or equivalently $j=l$ but $i\neq k$), and exchanged adjacent-bond terms, pairs with $i=l$ but $j\neq k$ (or equivalently $j=k$ but $i\neq l$), in terms of r_{jl} (or r_{ik}). Dashed line: $(\overline{\sigma}^{\mathrm{N\text{-}AD}})$ nonadjacent-bond terms, pairs with $i\neq k$ but $j\neq l$, in terms of $r_{\min}=\min(r_{ik},r_{jl})$. All distances are in units of d_{HS}.

the Kubo-Greenwood conductivity. To that effect, in Fig. 3, we present the average contribution of the different terms in $\overline{\sigma}^{\mathrm{KG}}$ from ion pairs at distance r, normalized to $4\pi r^2$ as in the usual representation of the pair-distribution function $g(r)$ for a liquid; all distances are in terms of d_{HS}. A brief discussion of the various terms follows.

Both the "direct" and the "exchanged" RPM contributions are represented in terms of the only distance $r\equiv r_{ij}=r_{kl}$ in these contributions. They should decay with a functional dependence of at least $[rt(r)]^2$, i.e., $r^2\exp(-2\alpha r)$, which, being short ranged, guarantees the Ohmic character of these contributions to a local conductivity. Recall that in the case being considered $\alpha\cdot d_{\mathrm{HS}}=2$. We have found that the structure of the RPM contribution is indeed dominated by the pair-distribution function and the squared hopping elements, while the r dependence induced by the wave-function structure $|\phi_m(i)|^2|\phi_n(j)|^2$ produces only a smooth modulation of the $g(r)[rt(r)]^2$ factor. In contrast, the range of the "exchanged" RPM with r is decreased by the averaging of $\phi_m^*(i)\phi_n(j)\phi_m(j)\phi_n^*(i)$; that is, the wave function contribution takes positive and negative values in the averages over the disordered ionic structures in our MC simulations, causing a faster decay than that of the RPM contribution in the vapor, and making the contribution nearly negligible at all distances in the dense liquid.

The contributions to $\overline{\sigma}^{\mathrm{KG}}$ from adjacent pairs are represented in terms of the distance $r\equiv r_{ik}$ between the extreme ions in the triplet. These terms should decay with a functional dependence of at least the self-convolution of $rt(r)$, i.e., $r^4\exp(-\alpha r)$ for large r. Moreover, the average over the disordered ionic positions once again (as in the second term) produces an extra decay factor, from the cancellation of positive and negative values of $\phi_m^*(i)|\phi_n(j)|^2\phi_m(k)$. We have not found a simple explanation for the systematically negative values of these contributions, which arises from the combination of the ionic correlations, in the term $(\mathbf{r}_{ij}\cdot\hat{\mathbf{u}})(\mathbf{r}_{jk}\cdot\hat{\mathbf{u}})$, and from the electronic structure, in the term $\phi_m^*(i)\phi_m(k)$, near the Fermi level; none of the signs involved are predeterminable. The separation of such adjacent-pair contributions into "direct" and "exchanged" terms, as is done in Table I is avoided in Fig. 3, where the sum is given, since the exchanged contribution is always very small.

Finally, the contribution from nonadjacent pairs is represented in terms of the minimum distance between ion pairs for which a hopping element does not appear, $r\equiv\min(r_{ik},r_{jl})$. In this case there is no decaying factor such as one proportional to $t(r)$ to guarantee that its contribution to the conductivity is local and Ohmic. Nevertheless, the figure shows that the averaging over the ionic disorder very effectively cancels contributions beyond a second-neighbor shell of these current-current correlations between distinct, i.e., non adjacent, bonds. In contrast, in a crystalline system at $T=0$, this last term would have correlations which are maintained, without decay, for arbitrary bond separation. The sign of this contribution is also not predeterminable.

In addition to the dependences shown in Fig. 3, there can also be possible effect of quantum decoherence, induced by the (classical) movement of the ions; such an effect would only be important if its decoherence length were shorter than the disorder-induced decay of the contributions to $\overline{\sigma}^{\mathrm{KG}}$. The full sample quantum coherence assumed in Eqs. (3) and (4) might be regarded as an unrealistic assumption in a hot fluid metal. However, the strong disorder, leading to the decays observed in Fig. 3, give an effective decoherence length $\lambda_D\alpha\approx 1$. Such a value may be closer to reality, for our application, than the RPM assumption $\lambda_D\alpha\ll 1$. A quantitative calculation of λ_D is beyond the scope of our simple TB-HS model, since it would require specifying the electron-ion (pseudo) potentials, instead of using the simple parametrized form for the hopping element t_{ij}. To repeat, the factor of 3 discrepancy between the RPM and the KG results is a relatively mild one for a property changing by several orders of magnitude along the liquid-vapor coexistence curve. The difference between the local $\overline{\sigma}$ and global $\langle\sigma\rangle$ versions is only appreciable in the expanded liquid regime $\rho d_{\mathrm{HS}}^3\leqslant 0.28$; however, it becomes a qualitative difference along the vapor branch, with a difference of many orders of magnitude between the smooth decay of the local versions ($\overline{\sigma}^{\mathrm{KG}}$ and $\overline{\sigma}^{\mathrm{RPM}}$) and the rapid fall of the global ones ($\langle\sigma\rangle^{\mathrm{KG}}$ and $\langle\sigma\rangle^{\mathrm{RPM}}$) as the system approaches the percolation threshold; the effect is shown in Fig. 2.

IV. CONCLUSIONS

The most important conclusion we draw, from comparing the experimental data for cesium and the present results, is that the TB-HS model contains the most important aspects of the electronic conduction in real hot fluid metals, despite its simplicity. The model, with a simple TB band for noninteracting electrons producing the only cohesive energy and the simplest HS repulsion between the ion cores, has been considered an oversimplification: it neglects the effects of

electron-electron interactions and hence of a possible Mott transition to an insulating phase, it fails to treat the realistic electron-ion pseudopotential (i.e., the realistic density of electronic states), and does not contain a realistic form of the effective ion-ion interaction (which produces the vapor-liquid condensation). However, the results presented here show that good (semiquantitative) agreement exists between σ_{exp} and the TB-HS model results: from a good theoretical treatment of the electrons in the disordered matrix of the TB orbitals, and an adequate representation of the ionic correlation structure leading to the appropriate distribution of hopping elements. Oversimplifications in the theoretical treatment of such features, ones intrinsic to the model, are much more dangerous than the simplicity of the model itself. For instance, the earliest calculations of σ in the TB-HS model were the result[6] of an extremely strong version of the RPM, one which assumes perfect delocalization of the electrons (i.e., $|\phi_n(i)|^2=1/N$), so that Eq. (8) is only a function of the density of states at the Fermi level and the average of $\langle(t_{ij}r_{ij})^2\rangle$. That average was then estimated assuming hard-sphere correlations among the ions. Such simplifications, of the effect of ionic disorder on the electrons and on the nature of the ionic correlations, result in a qualitative error for the predictions of $\sigma(\rho)$; in fact, leading to a conductivity increase at modest but non-negligible ρ. In our previous work,[3] we proved that such a qualitative failure may be corrected, within the noninteracting scheme of the TB-HS model, with the inclusion of the self-consistent ionic clustering and also with the use of the true electronic wave functions for each ionic configuration, unless the ionic density is extremely low (where conductivity measurements are experimentally inaccessible). In our $\overline{\sigma}^{\mathrm{RPM}}$ we include both of the above mentioned effects and obtain the decreasing conductivity at low density, but we still have to introduce the percolative character of the electronic conduction to obtain its physically correct behavior for the vapor branch of the coexistence curve. As an aside, there is no doubt that the electron-electron interaction does become important at extremely low densities.

On the other hand, apparently extremely strong assumptions, on the quantum decoherence, imposed in the KG and the RPM approaches, only lead to relatively mild differences in the estimates for σ, obtained using both the local and the global approaches. A detailed analysis of the contributions to $\overline{\sigma}^{\mathrm{KG}}$, in terms of separation between the current-correlated bonds, gives a clear insight into the role of disorder, which turns any quantum coherence beyond the second-neighbor distance into an irrelevance; such a detailed insight is not possible in the global result $\langle\sigma\rangle^{\mathrm{KG}}$. The subtle difference between the classical (fully incoherent) percolation, given by $\langle\sigma\rangle^{\mathrm{RPM}}$, and the quantum percolation (coherence over the entire sample), in $\langle\sigma\rangle^{\mathrm{KG}}$, seems to be a minor effect compared with the respective local versions $\overline{\sigma}^{\mathrm{RPM}}$ and $\overline{\sigma}^{\mathrm{KG}}$. Thus, the correlation structure of the ionic matrix, creating easy paths for the delocalization of the electrons, is the most important aspect of the disorder in the system; it cannot be replaced by an empirical distributions of the hopping elements without resulting in qualitative changes in the electrical conductivity. This is a warning for other studies of electronic systems with model distributions of disorder, the choice of uncorrelated disordered elements in the electronic Hamiltonian may introduce a strong unrealistic bias into the results.

Given the extreme simplicity of the TB-HS model, the exact solution of the electronic Hamiltonian, to drive the MC simulations for the ions, requires a heavy but feasible computational effort. The size of our samples, with $N=256$ electrons and the same number of ions, seems to be close to the minimum size required to make certain that the macroscopic limit of an intrinsic electrical conductivity is obtained from averaging over the variety of disordered equilibrium ionic configurations. Also, that size seems to be large enough to control the empirical coarsening of the δ function in Eq. (3) and to make conductance calculations roughly independent of contact details, when using Eq. (4). On the other hand, we have shown that there is no easy short cut to the full solution of the electronic Hamiltonian, for the above N, and to the computer simulation of ionic configurations, since any approximation on these aspects may easily change the qualitative behavior of the predicted conductivity. Any attempt to generalize towards a more realistic description in terms of electron-ion pseudopotentials, and an inclusion of electron-electron interaction effects, would face an apparently unbearable computational effort, in order to run computer simulations near the critical vapor-liquid region with the exact solution of the electronic density for many millions of ionic configurations.

Finally, we comment that the use of glue-model treatments for the (nonpair additive) effective interactions among ions, induced by the electronic delocalization, may offer a solution to the problems discussed in the previous paragraph. We have explored a self-consistent glue-model treatment for the TB-HS model elsewhere.[3] On the basis of previous work and the present paper, using our original approach $\overline{\sigma}^{\mathrm{RPM}}$ yields conductivity results which agree whether they are based on using glue-derived configurations (previous work) or based on those from the exact energies (this paper). There are, however, some discrepancies at the lowest vapor densities, where configurational differences seem to be most important. Another comparison of glue model based results and exact-based ones has been carried out[5] for thermodynamic and structural results of the TB-HS model, the conclusions are in agreement with those above. Therefore, it has been verified that a suitable glue model, based on typical configurations of the system to be studied, is able to give an adequate description of the ionic structures for hot metallic fluids, with an enormous reduction in the computational effort. Thus, it appears feasible to extend such glue-model treatments to metallic fluids described with more realistic electronic Hamiltonians. With such a treatment, it might become possible to find the liquid-vapor coexistence of such fluids and to evaluate the ionic correlations along that coexistence, using a large number of ions, with a computational effort comparable to that for simple fluids.

ACKNOWLEDGMENTS

This work has been supported by the Dirección General de Investigación (MCyT) of Spain, under Grant No. BFM2001-1679-C03.

[1] N. F. Mott, *Metal-Insulator Transitions* (Taylor and Francis, London, 1997), p. 237.
[2] M. Reinaldo-Falagán, P. Tarazona, E. Chacón, and J. P. Hernandez, Phys. Rev. E **60**, 2626 (1999).
[3] M. Reinaldo-Falagán, P. Tarazona, E. Chacón, E. Velasco, and J. P. Hernandez, Phys. Rev. B **67**, 024209 (2003).
[4] S. Jüngst, B. Knuth, and F. Hensel, Phys. Rev. Lett. **55**, 2160 (1985); F. Hensel and W. W. Warren, Jr., *Fluid Metals* (Princeton University Press, Princeton, 1999), p. 194.
[5] E. Chacón, P. Tarazona, M. Reinaldo-Falagán, E. Velasco, and J. P. Hernandez, Phys. Rev. B **71**, 024204 (2005), the following article.
[6] T. Koslowski, D. G. Rowan, and D. E. Logan, Ber. Bunsenges. Phys. Chem. **100**, 101 (1996).
[7] R. Redmer, H. Reinholz, G. Röpke, R. Winter, F. Noll, and F. Hensel, J. Phys.: Condens. Matter **4**, 1659 (1992).
[8] G. Franz, Ph.D. thesis, Philipps-Universität, Marburg, 1980.
[9] D. E. Logan and P. G. Wolynes, Phys. Rev. B **29**, 6560 (1984); J. Chem. Phys. **85**, 937 (1986); D. E. Logan and M. D. Winn, J. Phys. C **21**, 5773 (1988).
[10] R. Kubo, J. Phys. Soc. Jpn. **12**, 570 (1957); D. A. Greenwood, Proc. Phys. Soc. Jpn. **71**, 585 (1958).
[11] N. K. Hindley, J. Non-Cryst. Solids **5**, 17 (1970).
[12] A. Bastin, C. Lewiner, O. Betbeder-Matibet, and P. Nozieres, J. Phys. Chem. Solids **32**, 1811 (1971); B. K. Nikolić, Phys. Rev. B **64**, 165303 (2001).
[13] N. E. Cusak, *The Physics of Structurally Disordered Matter* (Adam Higler, Sussex, 1987), p. 192.
[14] T. Guhr, A. Müller-Groeling, and H. A. Widenmüller, Phys. Rep. **299**, 189 (1998).
[15] Such a recovery of Ohm's geometrical scaling of the conductance, in a formalism which exclusively accounts for coherent scattering, has been previously noticed in a quite different context by M. J. Calderón, J. A. Vergés, and L. Brey, Phys. Rev. B **59**, 4170 (1999).
[16] S. Datta, *Electronic Transport in Mesoscopic Systems* (Cambridge University Press, Cambridge, 1995); J. A. Vergés, Comput. Phys. Commun. **118**, 71 (1999).
[17] R. Redmer and W. W. Warren, Phys. Rev. B **48**, 14892 (1993).